

Final Technical Report for
U.S. Geological Survey
National Earthquake Hazard Reduction Program
Award No. 08HQGR0048

Spontaneous Dynamic Rupture Propagation with Off-Fault Plastic Yielding, Tensile Crack Generation, and Damage Rheology and the Effects on Ground Motion

Benchun Duan, PI

Department of Geology & Geophysics
Texas A&M University
College Station, TX 77843-3115

Tel: 979-845-3297
Fax: 979-845-6162
Email: duan@geo.tamu.edu

Term of Award: February 1, 2008 - January 31, 2009
No-cost Extension through January 31, 2010
Final Report Submitted: April 29, 2010

The views and conclusions contained in this document are those of the author and should not be interpreted as necessarily representing the official policies, either expressed or implied, of the U. S. Government.

ABSTRACT

We extend our explicit finite element method for rupture dynamics modeling to include several off-fault damage mechanisms, including off-fault plastic yielding, damage rheology with reduction in elastic constant, and tensile crack generation. We examine distributions of off-fault damage due to dynamic rupture on faults and their effects on rupture propagation and near-field ground motion. We find that off-fault damage around a fault kink (a change in fault strike) , generated by a rupture propagating from a more favorable segment to a less favorable segment, significantly reduces rupture speed. Extensive off-fault damage is associated with the kink and inelastic strain tends to localize into discrete bands, suggestive of the development or mobilization of secondary faults. High-frequency radiations from the kink are reduced significantly above several Hz by off-fault damage. We also find that asymmetric damage around active faults observed in the field does not necessarily indicate unilateral rupture propagation along a bimaterial interface. Rather, bilateral rupture propagation along the bimaterial interface can generate the asymmetric damage pattern over repeated earthquakes. Different mechanisms of off-fault damage can have different effects on rupture propagation and near-field ground motion, though they all tend to reduce rupture speed and peak ground velocity.

1. INTRODUCTION

Geological observations (e.g., Chester and Chester, 1998; Dor et al., 2006) have shown that a fault zone typically consists of a relatively thin principal slip zone surrounded by a damage zone with a width of several hundred meters (Ben-Zion and Sammis, 2003). Seismic trapped wave studies (e.g., Li et al., 1990; Ben-Zion et al., 2003) and InSAR data analyses (e.g., Fialko et al., 2002) reveal that seismic velocity and rock rigidity within a fault zone are reduced significantly (e.g., velocity reduction up to 50%) relative to surrounding, undamaged wall rock. These compliant, damaged fault zones are most likely caused by large dynamic stress perturbations associated with past earthquake ruptures. Theoretical analyses on the stress field near the tip of a steadily propagating rupture suggest that stresses elastically predicted near the rupture front can be large enough to cause failure of off-fault material based on a Coulomb failure criteria, particularly near the limit rupture speed (e.g., the Rayleigh wave speed for Mode II rupture) (Poliakov et al., 2002; Rice et al., 2005). Failure of off-fault material in turn will affect rupture propagation on the fault through the stress field, including rupture speed and slip velocity. The two-way interaction between rupture propagation and off-fault damage can be studied by spontaneous, dynamic rupture models.

In this project, we incorporate various off-fault damage mechanisms proposed for rock in literature into spontaneous, dynamic rupture models to examine their effects on rupture propagation and seismic wave radiations (thus ground motion). Off-fault damage mechanisms proposed in literature include plastic yielding (e.g., Andrews, 2005), damage rheology (e.g., Lyakhovskiy et al., 1997), and tensile crack generation (Dalguer et al., 2003). Plastic yielding may be considered as a continuum representation of brittle failure that dominates in the upper crust. But reduction in elastic constants and volumetric plastic strain are generally left out in this

mechanism. Damage rheology normally takes into the degradation of elastic moduli into account. Tensile crack generation involves energy dissipation due to absolute tensile stress that is likely occur near the ground surface during a dynamic event. Implementation of the three damage mechanisms in a finite element method becomes increasingly more difficult from plastic yielding, to damage rheology, and to tensile crack generation. We devote efforts to each of the three mechanisms in the period of this project, with an emphasis on the first two. Given the level of complexity in spontaneous rupture models with off-fault damage, we work in a two-dimensional, plane-strain framework in this project.

2. METHOD

We expand our explicit finite element method (FEM) code EQdyna to incorporate off-fault damage mechanisms into spontaneous, dynamic rupture models. The earlier version of the code were developed for elastodynamic analysis in which off-fault response is assumed to be linearly elastic. The basic formation of EQdyna for elastodynamic analysis is as follows: After discretizing the space domain into non-overlapping elements, the standard FEM formation for an elastodynamic problem with viscous damping leads to a semidiscrete (time is left continuous) matrix equation $\mathbf{M}\mathbf{a} + \mathbf{C}\mathbf{v} + \mathbf{K}\mathbf{u} = \mathbf{F}$, where \mathbf{M} is the mass matrix, \mathbf{C} is the viscous damping matrix, \mathbf{K} is the stiffness matrix, \mathbf{F} is the vector of applied forces, and \mathbf{u} , \mathbf{v} , \mathbf{a} are the displacement, velocity and acceleration vectors, respectively. We use the central difference time integration method with lumped, diagonal mass matrix \mathbf{M} to solve the above equation. Thus, the method is explicit and conditionally stable. For computational efficiency, we employ quadrilateral elements in two dimensions and hexahedral elements in three dimensions with one-point quadrature. One point quadrature requires a scheme to suppress hourglass modes of deformation and we adopt the method proposed by Kosloff and Frazier [1978]. The crucial feature of a dynamic FEM for modeling spontaneous earthquake rupture is implementation of the fault boundary condition. We use a version of the traction-at-split-node (TSN) scheme proposed by Day et al. (2005) with the linear slip-weakening friction law to implement fault boundaries.

For off-fault plastic yielding, we use a Mohr-Coulomb yield criterion given by $\tau \leq c - \sigma_n \tan \phi$, where τ and σ_n are shear and normal (positive in tension) stresses in any orientation at a point and c and ϕ are cohesion and the internal frictional angle, respectively. In 2D plane strain analysis with relevant stress components in the x, y plane, the criterion can be expressed as $\sqrt{\sigma_{xy}^2 + [(\sigma_{xx} - \sigma_{yy})/2]^2} \leq c \cos \phi - [(\sigma_{xx} + \sigma_{yy})/2] \sin \phi$. When stress state at a point in the medium violates the criterion, the shear stress components σ_{xy} and $(\sigma_{xx} - \sigma_{yy})/2$ are reduced by a common factor while there is no change in mean stress. After the adjustment, the stress state meets the criterion with the equal sign being used in the criterion. The increment of the plastic strain tensor $\delta \boldsymbol{\varepsilon}_{ij}^p$ can be calculated from the adjustment to each stress component $\delta \sigma_{ij}$ and shear modulus G by $\delta \boldsymbol{\varepsilon}_{ij}^p = \delta \sigma_{ij} / G$. The magnitude of plastic strain (permitting no plastic dilation) at a time can be calculated by $\boldsymbol{\varepsilon}^p = \sqrt{[(\boldsymbol{\varepsilon}_{xx}^p - \boldsymbol{\varepsilon}_{yy}^p)/2]^2 + (\boldsymbol{\varepsilon}_{xy}^p)^2}$.

For damage rheology, we use the continuum damage rheology model proposed by Lyakovsky et al. (1997). In this model, the constitutive relation is expressed as

$$\sigma_{ij} = \left(\lambda - \gamma \frac{\sqrt{I_2}}{I_1} \right) I_1 \delta_{ij} + \left(2\mu - \gamma \frac{I_1}{\sqrt{I_2}} \right) \varepsilon_{ij}^e, \text{ where } \lambda, \mu \text{ are Lamé constants, } I_1 = \varepsilon_{kk}^e \text{ is the first}$$

strain invariant of elastic strain tensor ε_{ij}^e , $I_2 = \varepsilon_{ij}^e \varepsilon_{ij}^e$ is the second strain invariant, and γ is the additional elastic modulus determined on the loss of convexity of rocks. The equation for damage evolution is

$$\frac{d\alpha}{dt} = -C \frac{\partial F}{\partial \alpha}, \text{ where } C \text{ is a state variable representing the nonnegative local entropy production and } F \text{ is Helmholtz free energy. } F \text{ is approximated by elastic energy } U \text{ in the}$$

proposed model (Lyakovsky et al., 1997), which can be calculated as

$$U = \frac{1}{\rho} \left(\frac{\lambda}{2} I_1^2 + \mu I_2 - \gamma I_1 \sqrt{I_2} \right), \text{ where } \rho \text{ is material density.}$$

The above two mechanisms of off-fault damage has been implemented in the 2D version of EQdyna. We apply off-fault plastic yielding to examine effects of off-fault damage on dynamic rupture through a fault kink and on seismic radiation from the kink, and to explore asymmetric damage along a bimaterial interface. We also examine how damage rheology may affect rupture propagation and near-field ground motion by working on planar fault models. Results from these studies are reported in the next section.

Among methods using FEM to model crack generation and evolution in literature (e.g., Belytschko et al., 2003), we work on enrichment methods, specifically extended FEM (XFEM) (e.g., Belytschko and Black, 1999) to include off-fault tensile crack generation. XFEM models discontinuities in a continuum body without need of remeshing for time evolution of cracks. In XFEM, an enriched solution is superimposed on the original finite element mesh to obtain the solution for a continuum body physically including cracks, while the original finite element mesh can remain the same even after cracks initiate and propagate. The basic approximation for displacement, $\mathbf{u}(\mathbf{x})$, in XFEM is

$$\mathbf{u}(\mathbf{x}) = \mathbf{u}^{FE}(\mathbf{x}) + \mathbf{u}^{enrichment}(\mathbf{x}) = \sum_{I=1}^n N_I(\mathbf{x}) \mathbf{u}_I + \sum_{J=1}^m N_J(\mathbf{x}) \Phi_J(\mathbf{x}) \mathbf{q}_J,$$

where \mathbf{u}_I is displacement at Node I, \mathbf{q}_J is the enriched degree of freedom (DOF) at Node J, N_J is the shape function, and $\Phi_J(\mathbf{x})$ is the enrichment function. Here, $\Phi_J(\mathbf{x})$ are used to increase the order of completeness can have different forms according to whether the location of Node J belongs to set of nodes for elements completely cut by crack, K_0 , or belongs to the set of nodes for element(s) surrounding Crack tip j ($j = 1, 2$), K_j . Challenges remain in XFEM for dynamic crack generation and propagation. One of the challenges is to determine the path for crack propagation. The second challenge is the complexity in numerical integration for the elements cut by crack as well as the elements including crack tips. Local remeshing, e.g., element partition, in the elements including crack and crack tips still is need to determine the quadratures for numerical integration. The third challenge is the development of explicit solution for XFEM. Stability study in explicit solutions is still an ongoing research topic. Because of these challenges associated with this newly emerged FEM method for crack generation and propagation, more

efforts are needed in the future to apply it to off-fault tensile crack generation during dynamic earthquake ruptures.

3. Main RESULTS: Dynamic rupture, off-fault damage distribution, and near-field ground motion

We work on several seismologically/geologically significant problems to examine off-fault damage on dynamic rupture and near-field ground motion, mainly using off-fault plastic yielding and damage rheology. We report main results in this section.

3.1. Inelastic strain distribution and seismic radiation from dynamic rupture of a kinked fault

We examine how off-fault plastic yielding affects rupture propagation through a fault kink and near-field particle velocity, and how inelastic strain is distributed around the fault kink. Our fault is a 2D right-lateral strike-slip fault consisting of two straight segments, with a change in strike between the two segments (Figure 1). We only discuss a case with the change of 10° in strike here. We consider a uniform pre-stress field with $\sigma_{xx} = \sigma_{yy} = -100MPa$ and

$\sigma_{xy} = 45MPa$. In this stress field, the left segment of the fault occupies a plane of maximum shear stress and the right segment is less favorable for rupture propagation compared with the left one. We assume a homogeneous medium to isolate fault kink effects, with density of 2700 kg/m^3 , P- and S- wave velocities of 5196 m/s and 3000 m/s , respectively, internal frictional and cohesion of 0.75 and 0 MPa , respectively. Static and dynamic frictional coefficients in a linear slip-weakening law are 0.6 and 0.3 , respectively, with a critical slip distance D_0 of 0.15 m . We test two element sizes (near the fault) of 5 m and 2.5 m . For the reference calculation with off-fault elastic response, we set cohesion to be a very large number (e.g., 10^{30} MPa) to prevent yielding from occurring.

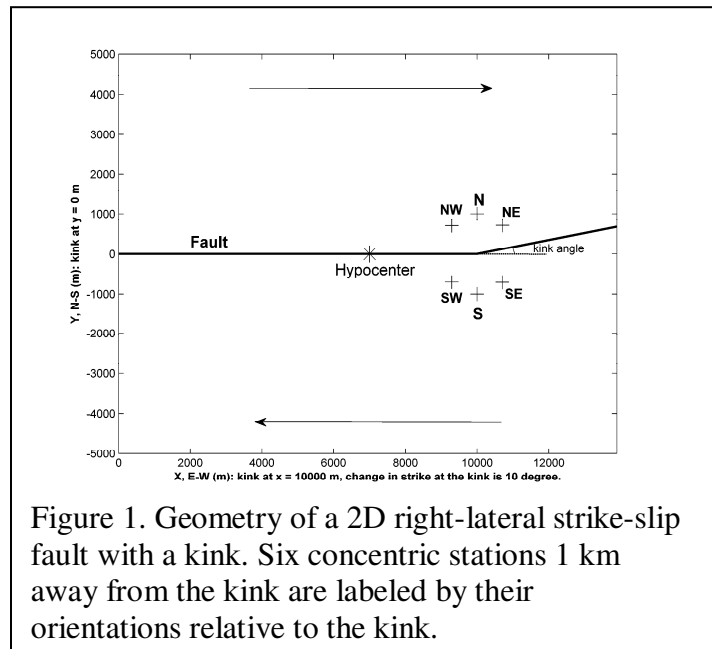


Figure 1. Geometry of a 2D right-lateral strike-slip fault with a kink. Six concentric stations 1 km away from the kink are labeled by their orientations relative to the kink.

Extensive plastic strain is associated with the change of strike (the kink) and occurs on the extensional side of the fault (i.e., σ_{xx} being less compressive due to rupture) (Figure 2). Plastic strain associated with the kink tends to localize into discrete bands. One long, narrow band of strong plastic strain originates from the kink and extends more than 2 km in the SEE direction, suggestive of the development or mobilization of one or more secondary faults during the dynamic event that helps to accommodate flow around the sharp change in the strike of the main fault. Although numerically simulating the above off-fault inelastic strain localization is challenging, the number, location and general shape of the plastic strain bands in this model are essentially grid-size independent, as evidenced by the results from the two element sizes.

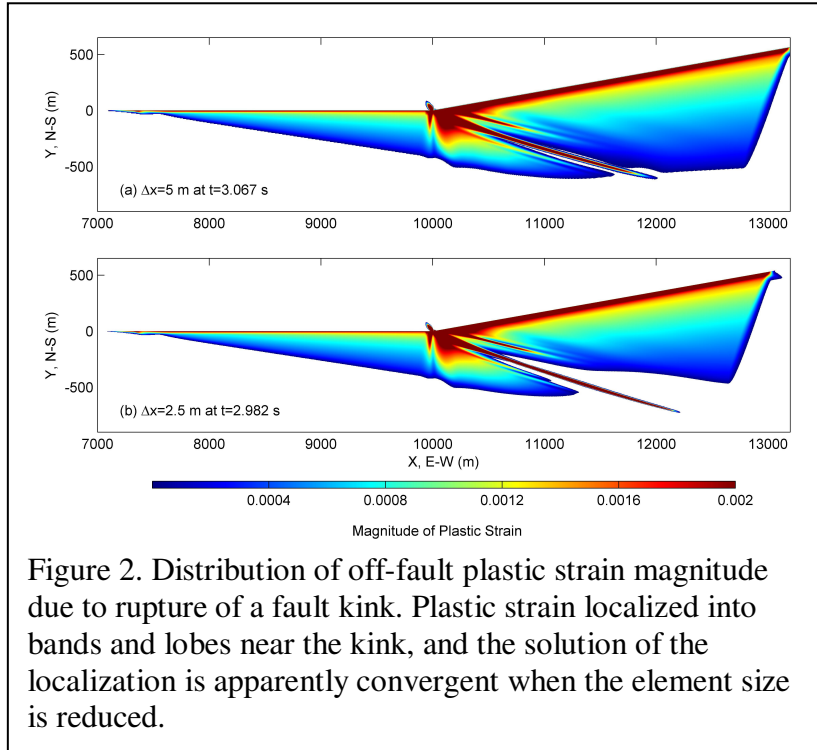


Figure 2. Distribution of off-fault plastic strain magnitude due to rupture of a fault kink. Plastic strain localized into bands and lobes near the kink, and the solution of the localization is apparently convergent when the element size is reduced.

Off-fault plastic yielding significantly reduces rupture speed upon passage through the fault kink (Figure 3). Rupture speed remains at a low level throughout the entire right segment, due to relatively extensive off-fault yielding associated with the segment. With elastic off-fault response,

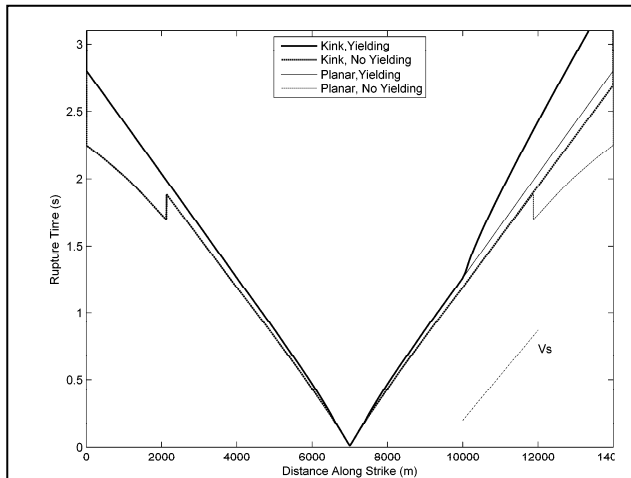


Figure 3. Rupture times along a kinked fault and a planar fault with off-fault elastic and elastoplastic responses.

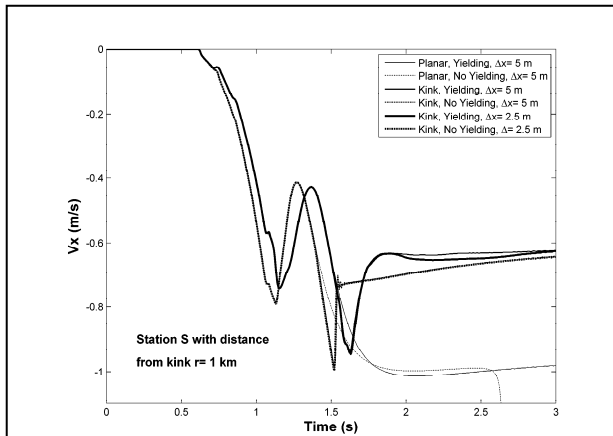


Figure 4. Particle velocity time histories at Station S (see Fig. 1). Velocity jumps beyond 1.5 s are caused by seismic radiation from the kink.

the kink with a change of 10° in strike does not cause obvious change in rupture speed. Off-fault plastic yielding reduces high-frequency radiations from the fault kink significantly above several Hz (Figure 4). This is evidenced by a ramp-like first motion caused by the kink radiation (the jump beyond 1.5 s) in the yielding case, while the first motion from the kink radiation in the elastic off-fault response case is essentially an instantaneous step function .

3.2. Asymmetric off-fault damage generated by bilateral ruptures along a bimaterial interface

Recent geological observations of damage asymmetry along sections of the San Andreas, San Jacinto, and Punchbowl faults in southern California have been used to argue for preferred unilateral rupture propagation along a bimaterial interface (e.g., Dor et al., 2006). In this project, we perform simulations of dynamic rupture along bimaterial interfaces with off-fault elastoplastic response. We find that bilateral ruptures on a bimaterial interface can generate an asymmetric off-fault damage pattern that is consistent with the above cited field observations. In other words, asymmetric damage pattern along active faults does not require unilateral ruptures. Rather, it can be caused by bimaterial effects on off-fault damage, even though ruptures themselves may be bilateral.

Figure 5 illustrates bimaterial effects on off-fault damage distribution due to one single earthquake event. Internal friction and cohesion in the models are 0.75 and 45 MPa, respectively. In the homogenous material model, density, P-wave., and S-wave velocities are 2670 kg/m^3 , 6000 m/s, and 3464 m/s, respectively. In the bimaterial model, softer material is on the positive-y (N-S) side of the fault and seismic velocities are reduced by 20%. With homogeneous material, off-fault inelastic strain occurs along two extensional quadrants of a 2D right-lateral strike-slip fault (along N-S $y = 0 \text{ km}$), and it is antisymmetric in the magnitude and extent with respect to the fault. Over multiple earthquake cycles, ruptures on the fault embedded in the homogenous medium will produce symmetric off-fault damage. On the other hand, off-fault inelastic strain is preferentially concentrated on one of the two extensional quadrants of the fault due to bimaterial effects (i.e., opposite normal stress changes along the two directions of rupture propagation, with tensile change being favorable for off-fault damage). Repeated bilateral earthquake ruptures on the bimaterial interface will generate asymmetric off-fault damage patterns as observed in field.

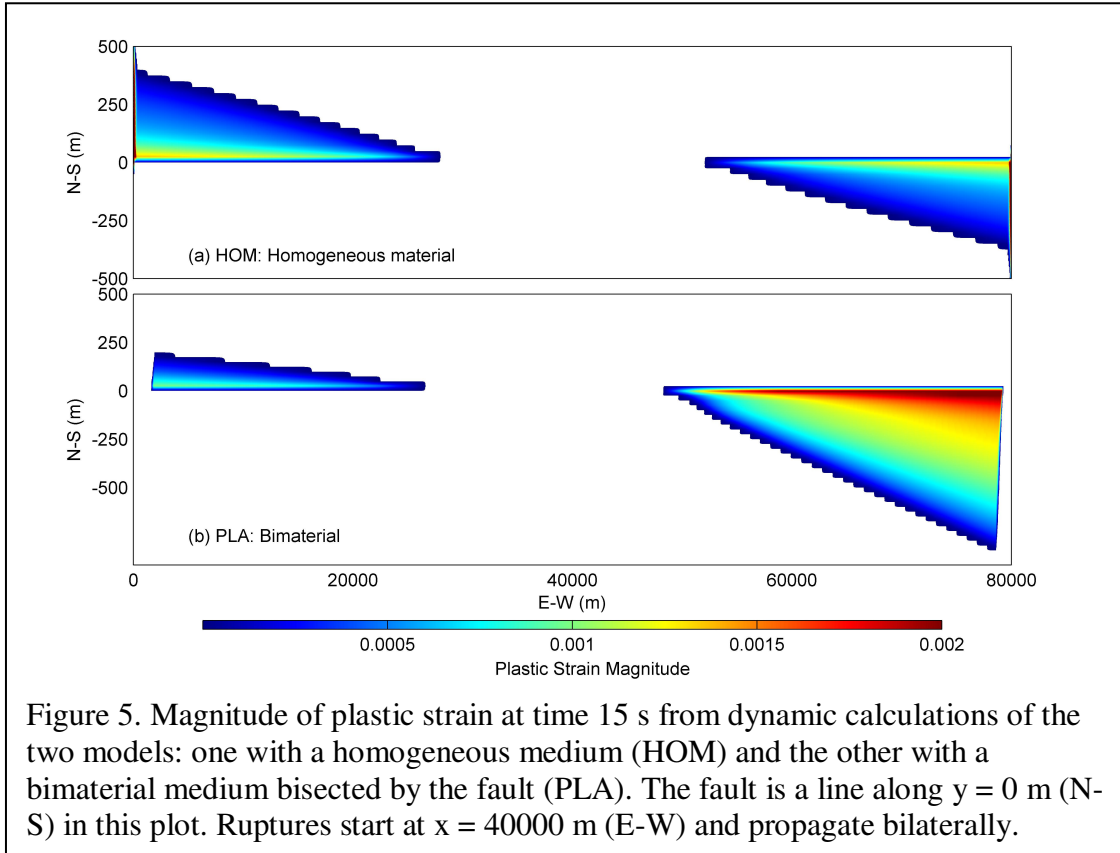


Figure 5. Magnitude of plastic strain at time 15 s from dynamic calculations of the two models: one with a homogeneous medium (HOM) and the other with a bimaterial medium bisected by the fault (PLA). The fault is a line along $y = 0$ m (N-S) in this plot. Ruptures start at $x = 40000$ m (E-W) and propagate bilaterally.

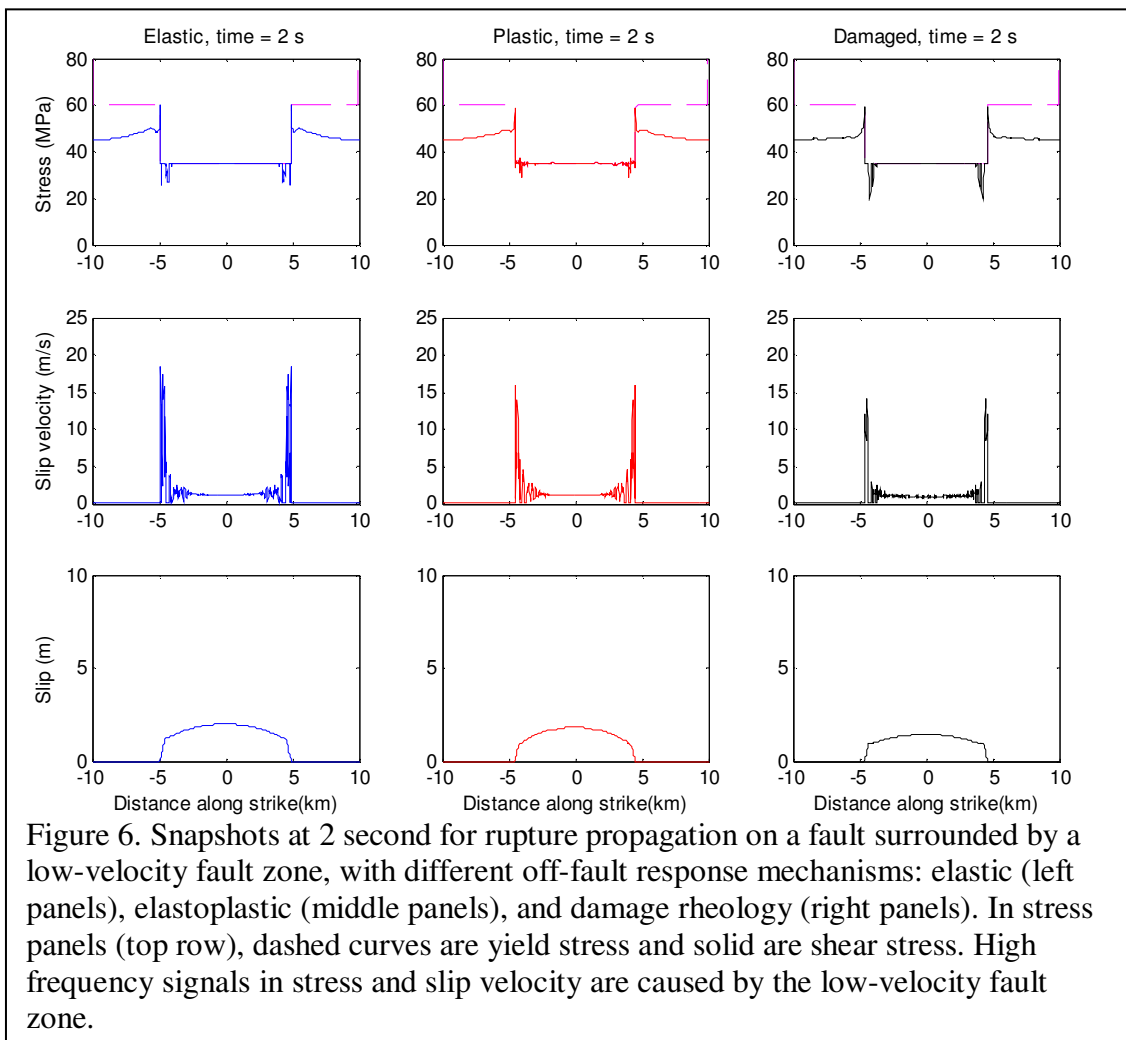
3.3. Comparing effects of different off-fault responses

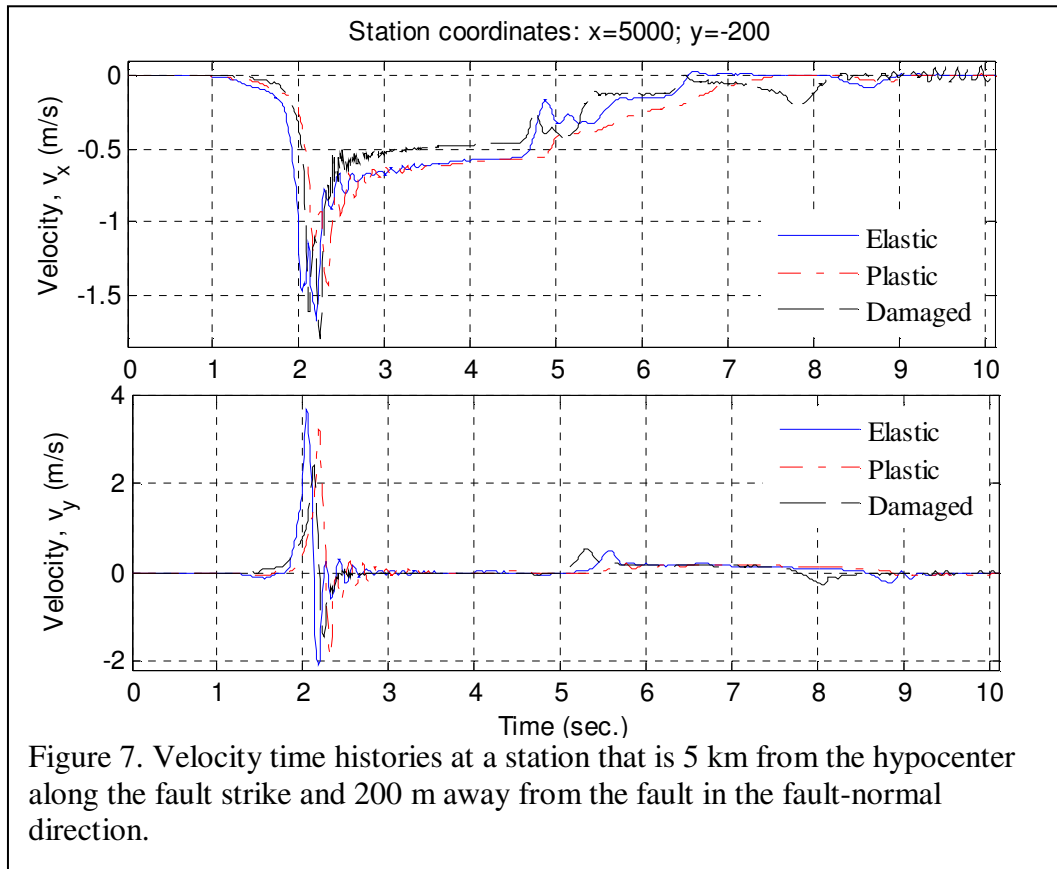
We work on models of a planar fault embedded in a low-velocity fault zone (LVFZ) within an otherwise homogeneous medium. The fault zone is 200 m wide with a reduction in seismic velocity of 40% relative to country rock. We compare rupture propagation and near-field particle velocity from calculations with different off-fault response mechanisms, including elastic, elastoplastic (plastic yielding), and damage rheology (with reduction in rigidity). Density in the model is uniform with a value of 2670 kg/m^3 . S-wave velocity of country rock is 3464 m/s. Internal friction and cohesion for country rock and the LVFZ are 0.85, 0.7, 1 MPa, and 0 MPa, respectively, in the elastoplastic calculation.

Figure 6 shows snapshots of rupture propagation on the fault with different off-fault response mechanisms. Rupture speed is fastest in the elastic case, slowest in the elastoplastic case, and in between in the damage rheology case. Peak slip velocity is reduced obviously by either off-fault plastic yielding or damage rheology from that of the elastic response and the reduction is more profound with damage rheology. These results indicate that plastic yielding and damage rheology have different effects on rupture speed and peak slip velocity: yielding has a larger effect on rupture velocity while a smaller effect on peak slip velocity, compared with damage rheology.

Effects on ground motion are compared in Figure 7. The station is 5 km away from the hypocenter along the fault strike and 200 m away from the fault in the fault-normal direction. Both fault-parallel (V_x) and fault-normal (V_y) components of peak ground velocity (PGV) are reduced by off-fault plastic yielding, compared with those from the elastic off-fault response. Damage rheology does not reduce fault-parallel PGV, but it reduces fault-normal PGV significantly (more profoundly than plastic yielding). These different effects on ground motion from different off-fault damage mechanisms are worth further exploration in the future.

We remark that damage level that can be achieved in a dynamic event based on the damage rheology model proposed by Lyakhovsky et al. (1997) is limited to moderate damage before loss of convexity. Further extension of the damage rheology model to higher damage levels (e.g., through addition of some plastic mechanisms) is needed for dynamic rupture simulations in the future.





REFERENCES CITED

- Andrews, D. J. (2005), Rupture dynamics with energy loss outside the slip zone, *J. Geophys. Res.*, 110, B01307, doi:10.1029/2004JB003191.
- Ben-Zion, Y. and C. G. Sammis (2003), Characterization of fault zones, *Pure Appl. Geophys.*, 160, 677-715.
- Ben-Zion, Y., Z. Peng, D. Okaya, L. Seeber, J. G. Armbruster, N. Ozer, A. J. Michael, S. Baris, and M. Aktar (2003), A shallow fault zone structure illuminated by trapped waves in the Karadere-Duzce branch of the North Anatolian Fault, western Turkey, *Geophys. J. Int.*, 152, 699-717.
- Belytschko, T., Black, T. (1999), Elastic crack growth in finite elements with minimal remeshing, *International Journal for Numerical Methods in Engineering*; 45(5), 601–620.

- Belytschko, T., Chen, H., Xu, J. and Zi, G. (2003), Dynamic crack propagation based on loss of hyperbolicity and a new discontinuous enrichment, *International Journal for Numerical Methods in Engineering*, 58, 1873–1905.
- Chester, F. M. and J. S. Chester (1998), Ultracataclasite structure and friction processes of the Punchbowl fault, San Andreas system, California, *Tectonophysics*, 295, 199-221.
- Dalguer, L. A., K. Irikura, and J. D. Riera (2003), Simulation of tensile crack generation by three-dimensional dynamic shear rupture propagation during an earthquake, *J. Geophys. Res.*, 108(B3), 2144, doi:10.1029/2001JB001738.
- Day, S. M., L. A. Dalguer, N. Lapusta, and Y. Liu (2005), Comparison of finite difference and boundary integral solutions to three-dimensional spontaneous rupture, *J. Geophys. Res.*, 110, B12307, doi:10.1029/2005JB003813.
- Dor, O, T. K. Rockwell, and Y. Ben-Zion (2006), Geological observations of damage asymmetry in the structure of the San Jacinto, San Andreas and Punchbowl faults in southern California: A possible indicator for preferred rupture propagation, *Pure Appl. Geophys.*, 163, 301-349, doi:10.1007/s00024-005-0023-9.
- Duan, B., and D. D. Oglesby (2006), Heterogeneous fault stresses from previous earthquakes and the effect on dynamics of parallel strike-slip faults, *J. Geophys. Res.*, 111, B05309, doi:10.1029/2005JB004138.
- Fialko, Y. et al. (2002), Deformation on nearby faults induced by the 1999 Hector Mine earthquake. *Science* 297, 1858-1862 .
- Kosloff, D., and G.A. Frazier (1978), Treatment of hourglass patterns in low order finite element codes, *Numerical and Analytical Methods in Geomechanics*, 2, 57-72.
- Li, Y. G., P. C. Leary, K. Aki, and P. E. Malin (1990), Seismic trapped modes in the Oroville and San Andreas fault zones, *Science*, 249, 763-766.
- Lyakhovskiy, V., Y. Ben-Zion, and A. Agnon (1997), Distributed damage, faulting, and friction, *J. Geophys. Res.*, 102, 27,635-27,649.
- Poliakov, A. N. B., R. Dmowska, and J. R. Rice (2002), Dynamic shear rupture interactions with fault bends and off-axis secondary faulting, *J. Geophys. Res.*, 107 (B11), 2295, doi:10.1029/2001JB00572.
- Rice, J. R., C. G. Sammis, and R. Parsons (2005), Off-fault secondary failure induced by a dynamic slip pulse, *Bull. Seismol. Soc. Am.*, 95 (1), 109-134, doi: 10.1785/0120030166.

BIBLIOGRAPHY OF PUBLICATIONS RESULTING FROM THIS WORK

- Duan, B. (2008), Asymmetric off-fault damage generated by bilateral ruptures along a bimaterial interface, *Geophys. Res. Lett.*, 35, L14306, doi:10.1029/2008GL034797.
- Duan, B., and S. M. Day (2008), Inelastic strain distribution and seismic radiation from rupture of a fault kink, *J. Geophys. Res.*, 113, B12311, doi:10.1029/2008JB005847.
- Zhong, J., and B. Duan (2009), Strain-dependent damage evolution and velocity reduction in fault zones induced by earthquake rupture, *Eos Trans. AGU*, 90(52), Fall Meet. Suppl., Abstract S21B-1721.